Genetic Deletion of Tissue Inhibitor of Metalloproteinase-1/TIMP-1 Alters Inflammation and Attenuates Fibrosis in Dextran Sodium Sulphate-induced Murine Models of Colitis

Peer-reviewed author version

Breynaert, Christine; de Bruyn, Magali; ARIJS, Ingrid; Cremer, Jonathan; Martens, Erik; Van Lommel, Leentje; Geboes, Karel; De Hertogh, Gert; Schuit, Frans; Ferrante, Marc; Vermeire, Severine; Ceuppens, Jan; OPDENAKKER, Ghislain & Van Assche, Gert (2016) Genetic Deletion of Tissue Inhibitor of Metalloproteinase-1/TIMP-1 Alters Inflammation and Attenuates Fibrosis in Dextran Sodium Sulphate-induced Murine Models of Colitis. In: JOURNAL OF CROHNS & COLITIS, 10(11), p. 1336-1350.

DOI: 10.1093/ecco-jcc/jjw101
Handle: http://hdl.handle.net/1942/23041

Journal of Crohn's and Colitis Advance Access published May 17, 2016

Manuscript Doi : 10.1093/ecco-jcc/jjw101

Genetic deletion of tissue inhibitor of metalloproteinase-1/TIMP-1 alters inflammation and attenuates fibrosis in dextran sodium sulphate induced murine models of colitis

Christine Breynaert[1,2], Magali de Bruyn[1,3], Ingrid Arijs[1,5], Jonathan Cremer[1,2], Erik Martens[3], Leentje Van Lommel[5], Karel Geboes[4], Gert De Hertogh[4], Frans Schuit[5], Marc Ferrante[1,6], Séverine Vermeire[1,6], Jan Ceuppens[2], Ghislain Opdenakker[3] and Gert Van Assche[1,6]

[1] Translational Research Center for Gastrointestinal Disorders (TARGID), Department of Clinical and Experimental Medicine, KU Leuven, Leuven, Belgium

[2] Laboratory of Clinical Immunology, Department of Microbiology and Immunology, KU Leuven, Leuven, Belgium

[3] Laboratory of Immunobiology, Department of Microbiology and Immunology, Rega Institute for Medical Research, KU Leuven, Leuven, Belgium

[4] Translational Cell and Tissue Research, Department of Imaging and Pathology, KU Leuven, Leuven, Belgium

[5] Gene Expression Unit, Department of Cellular and Molecular Medicine, KU Leuven, Leuven, Belgium

[6] Department of Gastroenterology and Hepatology, University Hospitals Leuven, KU Leuven, Leuven, Belgium

CB and MdB share first co-authorship

Short title: TIMP-1 deficiency in DSS colitis and fibrosis

Corresponding author:

Gert Van Assche, MD, PhD

University Hospitals Leuven, Department of Gastroenterology, Herestraat 49, 3000 Leuven

E-mail: gert.vanassche@uzleuven.be

Phone: +32 16 37 74 52

Fax: +32 16 3 44419

Conference presentations: ECCO Barcelona 2015 (poster presentation and oral presentation in Y-ECCO Basic Science Workshop), BWGE Brussels 2015 (oral poster presentation) and DDW Washington 2015 (poster presentation).

ABSTRACT

Background and aims: Increased levels of tissue inhibitor of metalloproteinase-1 (TIMP-1) have been detected in both inflammatory and fibrotic lesions in Crohn's disease. In a murine model of chronic inflammation, fibrosis was associated with an increase in TIMP-1 and inhibition of matrix metalloproteinase (MMP)-mediated degradation. We investigated the effect of TIMP-1 deficiency in acute and chronic murine models of colitis.

Methods: Colitis was induced via oral administration of dextran sodium sulphate (DSS) to B6.129S4-Timp1^{tm1Pds}/J knock-out (KO) and C57BL/6J wild-type (WT) mice. Levels of inflammation and fibrosis were assessed and gelatin zymographies and gene expression microarrays were performed.

Results: Compared to WT mice, TIMP-1 KO mice had higher inflammatory parameters after acute DSS administration and developed less fibrosis after chronic DSS administration. MMP-2 levels were increased in WT *versus* TIMP-1 KO mice with acute colitis, whereas a trend for higher proMMP-9 levels was observed in WT *versus* TIMP-1 KO mice with chronic colitis. In control conditions, several immune-related genes (e.g. *Ido1*, *Cldn8*) were differentially expressed between young TIMP-1 KO and WT mice, but to a lesser extent between older TIMP-1 KO and WT mice. In response to DSS, the gene expression pattern was significantly different between young TIMP-1 KO and WT mice, whereas it was similar in older TIMP-1 KO and WT mice.

Conclusions: TIMP-1 deficiency leads to differential expression of immune-related genes and to attenuated development of fibrosis. Unraveling the role of TIMP-1 in intestinal remodeling is necessary to develop more effective and more targeted therapeutic strategies for intestinal fibrosis.

Key words: TIMP-1, DSS, colitis, fibrosis

INTRODUCTION

Inflammatory bowel diseases (IBD), comprising Crohn's disease (CD) and ulcerative colitis (UC), are heterogeneous idiopathic inflammatory disorders of the intestine probably triggered by an inappropriate immunologic response to commensal gut microbiota in a genetically susceptible host[1]. IBD are disabling diseases, occurring mostly in young patients and often leading to a decreased quality of life because of recurrent inflammatory flares or complications such as perforating ulcers and fibrosis[2,3]. Chronic intestinal inflammation leads to tissue damage, subsequent tissue repair and an increased turnover of the extracellular matrix (ECM) with accumulation of excess ECM proteins, including collagens. Due to the transmural nature of the inflammatory process, fibrosis in CD patients leads to bowel wall thickening with narrowing of the lumen and eventually formation of strictures and stenosis. In UC patients, where inflammation is affecting the mucosal and submucosal layers, fibrosis develops with thickening of the muscularis mucosae and accumulation of ECM contributing to the shortening and the stiffening of the colon[4-6]. Fibrosis is a major clinical problem in IBD patients of whom more than thirty percent of CD patients evolve towards a distinct fibrostenosing phenotype. Up to eighty percent of all CD patients undergo surgery at least once during the course of their disease, most often for stricturing disease, and recurrence of stricture formation is common at the site of anastomosis[7-10]. However, until now, the time course, pathophysiology, specific treatment, and reliable biomarkers of intestinal fibrosis still need to be identified.

Whether fibrosis develops or not depends in part on the balance between ECM protein deposition and degradation. Fibrosis develops when excessive ECM accumulation occurs with failing of restoration of the normal tissue architecture[11]. Specific matrix metalloproteinases (MMPs), mainly collagenases and gelatinases, regulate collagen degradation. MMPs are zinc- and calcium-dependent ECM degrading endopeptidases that collectively have the capacity to degrade all types of ECM proteins and are secreted by a wide variety of cell types[12,13]. MMP activities are regulated by two major types of endogenous inhibitors: α2-macroglobulin and four tissue inhibitors of MMPs (TIMPs)[14,15]. TIMPs have some selectivity for specific MMPs, as TIMP-1 is the major inhibitor of MMP-

9, whereas TIMP-2 mainly blocks MMP-2. In several studies, an upregulation of MMPs in IBD[16-19], a disease-promoting role of MMP-9[20,21] and beneficial effects of metallobodies (neutralizing monoclonal antibodies against MMP active sites with TIMP-like activity)[22] in dextran sodium sulphate (DSS) colitis have been shown. An increased level of TIMP-1 protein has been reported in inflammatory and fibrotic lesions in CD[23,24]. In a murine model of chronic inflammation, fibrosis was associated with an increase in TIMP-1 levels and inhibition of MMP-mediated degradation[25]. These reports suggest a prominent role of MMPs and TIMPs in both tissue damage and remodeling in IBD.

The aim of this study was to investigate the effect of TIMP-1 deficiency on inflammation and fibrosis in murine colitis. To this end we used two DSS models of, respectively, acute and chronic colitis. Previously, we have shown that murine colitis induced by repeated cycles of DSS mimics the chronically relapsing inflammation underlying the complications of human CD and that this is an attractive model to study the connective tissue changes and intestinal fibrosis occurring in IBD[26]. We hypothesized that, in the absence of TIMP-1, more MMP activity and consequently more severe inflammation might occur on the one hand, whereas on the other hand more collagen degradation and less fibrosis would occur.

MATERIALS AND METHODS

Mice

Female 8-10 week old B6.129S4-Timp1^{tm1Pds}/J knock-out (KO) mice and C57BL/6J wild-type (WT) mice were bred at the Rega Institute for Medical Research, KU Leuven (Prof. Dr. G. Opdenakker). B6.129S4-Timp1^{tm1Pds}/J KO mice were initially obtained from The Jackson Laboratory (Bar Harbor, ME) in 2009 and since then bred under specific pathogen-free conditions in the animal facility with identical food and environmental conditions as the WT mice. The mice were maintained in accordance with institutional guidelines and the study was approved by the local ethics committee for animal experimentation of the University of Leuven (P134-2010 and P178-2011).

All mice in this study were confirmed for their TIMP-1 KO or WT genotype by PCR, as detailed in **supplementary table 1** and **supplementary figure 1**. In addition to KO status, we also carefully characterized the genetic background of the used mice, because in most studies of complex diseases this aspect is insufficiently addressed. A tail sample of 0.5-1.0 cm was collected from all mice at time of sacrifice and frozen at -80°C. Genomic DNA was extracted from the tail tips and background strain characterization was performed on a panel of 1449 SNP markers (Taconic, Renssealaer, NY, USA). The SNP markers are spread across the 19 mouse autosomes and the X chromosome at 5 Mbps intervals and are polymorphic between various strains of mice. The panel contains approximately four SNP markers per 5 Mbp interval. At least one of these four markers is informative in 85% of all possible combinations of major strains. In particular, 12 SNPs are polymorphic between C57BL/6J and C57BL/6N **(Supplementary table 2)**. An array of inbred and reference strain controls were also analyzed along with our samples. From 3 female B6.129S4-Timp1^{tm1Pds}/J and 4 female C57BL/6.WT mice, tail DNA was used to evaluate the purity of the strain lines. Data were analyzed by direct comparison of SNPs measured in each sample against a sample from a reference strain tested by the same method. Markers homozygous for the expected allele in the background to be quantified were scored as “1”. Markers heterozygous for the expected allele and another allele were scored as “0.5”.

Markers homozygous for another allele were scored as "0". The score for each marker was averaged to calculate the percent of the strain of interest in the background.

Induction of colitis

Acute colitis was induced by oral administration of 3 % DSS (35–50 kDa; MP Biomedicals, Illkirch, France) in the drinking water for 7 days followed by 2 days on normal drinking water (**Figure 1A**). Chronic DSS colitis was induced by 3 cycles of DSS administration as previously described[26]. One cycle of DSS comprised the induction of colitis by administration of DSS in drinking water for 7 days followed by a recovery period of two weeks with normal drinking water. This was repeated three times (**Figure 1A**). Based on previous experience, 1.75 % DSS in the drinking water was given during the first week of DSS administration, 2.00 % during the second and third cycle. Control mice (WT and TIMP-1 KO) received normal drinking water throughout the experimental time intervals.

Evaluation of colonic inflammation and histology

Animals were euthanized with sodium pentobarbital (Nembutal, Ovation Pharmaceuticals Inc. Deerfield, US). The Disease Activity Index (DAI) and macroscopic damage scores were calculated as previously described[26]. The entire colon was removed, cleaned, weighted and measured from the ileocaecal junction to anus. One part of the most infiltrated distal colon was fixed in 4 % formalin for histology analysis and Martius-scarlet-blue (MSB) staining, whereas other parts were snap-frozen for zymography analysis, hydroxyprolin assay and microarray analysis. Histology analysis was performed on paraffin-embedded, 5 µm-thick longitudinal and transverse sections stained with hematoxylin and eosin. The microscopic score of inflammation and histological active disease score were calculated as previously described[26]. Slides were scored by experienced pathologists (K.G. and G.D.H.) blinded to the experimental conditions.

Evaluation of fibrosis and chronic wound healing

Paraffin-embedded sections were stained using a MSB trichrome staining highlighting connective tissue changes[27,28]. Images were acquired using a Zeiss Axiovert 200 microscope, a Zeiss Axiocam MRc5 camera and the Zeiss Axiovision 4.7.1.0 software imaging system. The thickness of the mucosa and muscularis propria was calculated as the mean value of two different points per mouse on uniform horizontal cross sections of colon crypts using ImageJ[29]. To evaluate collagen content in tissues, a hydroxyprolin assay was performed as previously described[30].

Immunohistochemistry

Myeloperoxidase (MPO) staining was performed on paraffin-embedded sections with the use of the Leica Bond Max automated system (Leica Microsystems Belgium BVBA, Diegem, Belgium) and the Bond Polymer Refine Detection kit (DS9800, Leica). Briefly, slides were pre-treated with H2 buffer (AR9640, Leica) for 20 minutes. The slides were then incubated for 30 minutes with a rabbit anti-MPO polyclonal antibody (dilution 1/2000, A0398, Dako Belgium NV, Heverlee, Belgium). Thereafter, the slides were incubated with Leica polymer for 15 min, followed by DAB for 10 minutes and a hematoxylin counterstain for 5 minutes. MPO positive cells were counted by a gastrointestinal pathologist (GDH) in 2 representative high power fields (HPFs) per slide (one longitudinal and one cross-section). The average of MPO positive cells in 2 HPFs was used for statistical analysis.

Gelatin zymography

Gelatin zymography was used as described earlier[16,31] and in accordance with recent recommendations and standardizations[32]. The snap-frozen colon samples were prepurified as detailed elsewhere[33] and spiked with a known amount of a recombinant deletion mutant of human MMP-9 (that does not interfere with any mouse gelatinolytic enzyme). The spiking reference was included for quantitative standardization. In addition, to identify and qualitatively distinguish between the various forms of mouse MMPs, a standard of human gelatinase B multimers, monomers

and a deletion mutant was included on the analytical zymography gels. In this way the monomeric and multimeric forms, the proforms and activation forms of both mouse MMP-2 and MMP-9 were distinguished. Information about weight and protein concentration of all tissue samples was collected and enzyme levels were calculated relative to tissue amounts (fmol/mg).

Whole-transcript expression microarray analysis

Total RNA was extracted from snap frozen colon (Qiagen RNeasy Mini Kit cat # 74106) according to the manufacturer's guidelines. As previously described[26], total RNA (200 ng) was analyzed for the whole genome gene expression via mouse Gene 1.0 ST arrays (Affymetrix, Santa Clara, CAUSA), according to manufacturer's manual 4475209 Rev.B (Applied biosystems, CA) and 702808 Rev.6 (Affymetrix, CA). The microarray data were deposited at Gene Expression Omnibus under the series accession number GSE73424 (http://www.ncbi.nlm.nih.gov/geo/query/acc.cgi?token=mhcvwagsntifdad&acc=GSE73424) and were handled in accordance with the MIAME (Minimum Information About a Microarray Experiment) guidelines.

The microarray data were analysed using Bioconductor tools in R (http://www.r-project.org)[34]. The Affymetrix raw gene array data (.CEL files) were pre-processed (background correction, normalization and summarization) with robust multichip analysis to obtain a log2 expression value for each gene probe set using the implementation in the aroma.affymetrix R package[35]. Unsupervised complete-linkage hierarchical clustering, using Euclidian distance as metric, was performed to visualize gene (probe set)/sample relationship. The clustering results were visualized as a 2-dimensional heatmap with 2 dendograms, one indicating the similarity between samples and the other indicating the similarity between gene probe sets. For comparative analysis, linear models for microarray data (LIMMA)[36] was performed for all the gene probe sets present on the microarray to identify probe sets that are different between the groups, based on moderated *t*-statistics with Benjamini Hochberg false discovery rate (FDR) correction[37].

Statistical analysis

Statistical analysis and calculations were performed using GraphPad Prism 5.03 (GraphPad, La Jolla, CA, USA) and R (http://www.r-project.org). Data are represented as medians (25 % percentile, 75 % percentile) and the individual p-values for two groups were obtained using Mann-Whitney *U* testing (* $p<0.05$, ** $p\leq0.01$, *** $p\leq0.001$), unless annotated differently. Differences were considered statistically significant at $p<0.05$. Significance levels of the different groups compared with control mice without administration of DSS are shown above the corresponding group.

RESULTS

TIMP-1 KO mice are on a mixed C57BL/6J and C57BL/6N background

By genotyping of the mice used in this study, we confirmed that TIMP-1 KO mice generated indeed a smaller TIMP-1 gene product (200bp) in comparison with WT mice (393bp) (**Supplementary figure 1**). In addition, background characterization was performed on a panel of 1449 SNPs in both WT and TIMP-1 KO mice. According to 1449 SNP analysis data, the TIMP-1 KO mice were 99.17% of C57BL/6J recipient genome. Based on these calculations, TIMP-1 KO mice were on an acceptable generation equivalent of 7. Moreover, TIMP-1 KO mice displayed non-C57BL/6 character SNPs on the X chromosome and displayed both C57BL/6J and C57BL/6N character for the 12 SNPs that differentiate between these substrains. The presence of 3 of these 12 SNPs showed that TIMP-1 KO mice were partially on C57BL/6N background (**Supplementary table 2**). Two of the 3 SNPs could be linked to a specific gene: rs13478783 to *Snca* and rs4165065 to *Snap29*. WT animals were 99.93% of C57BL/6J recipient genome and displayed only C57BL/6 character.

Acute inflammation is impaired in absence of TIMP-1

The experimental set-up for induction of acute colitis is shown in **Figure 1A**. TIMP-1 KO mice recovered significantly faster after DSS administration compared with WT mice (relative weight at day 9: $p<0.001$) (**Figure 1B**). In line, the DAI was significantly lower in TIMP-1 KO mice compared with

WT mice after induction of acute colitis (p<0.001) (**Figure 1C**). Colon weight was significantly higher in TIMP-1 KO mice compared with WT mice after DSS administration (p<0.001) (**Figure 1D**). Colon length was significantly shorter in both WT and TIMP-1 KO mice after administration of DSS compared with control mice (p<0.001). Moreover, the colon of WT mice (5.8 cm (5.5 – 6.1)) was significantly shorter than the colon of TIMP-1 KO mice (6.3 cm (6.0 – 7.0)) after induction of acute colitis (p=0.012) (**Figure 1E**). The colon weight/length ratio and macroscopic damage score were significantly higher after induction of acute colitis in TIMP-1 KO mice compared with WT mice (p<0.001) (**Supplementary figure 2A and figure 2A**). In contrast, the histological inflammation score was not significantly different in WT and TIMP-1 KO mice after acute DSS administration (p=0.096) (**Figure 2B-C**). In addition, the spleen weight, used as a measure of systemic inflammation, was significantly higher after induction of acute colitis in TIMP-1 KO mice compared with WT mice (p=0.016) (**Figure 2D**). The spleen weight of TIMP-1 KO mice in control conditions was not significantly different from DSS-treated TIMP-1 KO mice (p=0.272) (**Figure 2D**).

Myeloperoxidase (MPO) positive cells were identified by immunohistochemistry (**Figure 3A**) and the average count of 2 representative HPFs was used for statistical analysis. After induction of acute colitis, increased numbers of MPO positive cells were observed in both WT and TIMP-1 KO mice compared to corresponding control mice (**Figure 3B**). However, no differences were observed between DSS exposed WT and TIMP-1 KO mice. Furthermore, we performed a MSB staining on colon sections to study connective tissue changes **(Supplementary figure 3A**). No differences were observed in DSS-treated TIMP-1 KO compared to WT mice (p=0.052) (**Supplementary figure 3B**).

Fibrosis and remodeling are reduced in TIMP-1 KO mice after induction of chronic colitis

Chronic colitis was induced by repeated administrations of DSS followed by a recovery period in order to study remodeling in absence of TIMP-1 (**Figure 1A)**. One WT mouse died during the third cycle of DSS administration. During the first cycle of DSS, all mice experienced weight loss. However, TIMP-1 KO mice recovered faster after this first week of DSS administration compared with WT mice,

and lost less weight during the second and third administration of DSS, resulting in a significant increased relative weight compared with WT mice after induction of chronic colitis (p=0.006) (**Figure 1B**). This correlated with a significantly decreased DAI (p=0.031) (**Figure 1C**), macroscopic damage score (p<0.001) (**Figure 2A**) and histological inflammation score (p=0.016) (**Figure 2B-C**) in TIMP-1 KO mice compared with WT mice after repeated cycles of DSS administration. Colon weight was higher in both WT and TIMP-1 KO mice after chronic administration of DSS (**Figure 1D**). The colon weight/length ratio was significantly lower in TIMP-1 KO mice compared with WT mice after 3 cycles of DSS (p=0.027) (**Supplementary figure 2B**), due to a significantly shorter colon in WT mice (6.8 cm (6.2 – 7.2)) compared with TIMP-1 KO mice (8.1 cm (7.5 – 8.5)) after induction of chronic colitis (p<0.001) (**Figure 1E**). Spleen weight was significantly higher in both WT and TIMP-1 KO mice after induction of chronic colitis (**Figure 2D**). Increased numbers of MPO positive cells were observed in both WT and TIMP-1 KO mice after induction of chronic colitis compared to corresponding control mice (**Figure 3A**). However, no significant differences were observed between DSS exposed WT and TIMP-1 KO mice (**Figure 3B**).

To quantify the amount of fibrosis, we measured the concentration of collagen in the colon using a hydroxyprolin assay. After chronic DSS administration, significantly lower amounts of collagen were detected in TIMP-1 KO mice compared with WT mice (p=0.003) (**Figure 4A**). Furthermore, the thickness of the muscularis propria, notably the external muscular layer, increased significantly in both WT and TIMP-1 KO mice after induction of chronic DSS colitis, although, it tended to be thinner in DSS exposed TIMP-1 KO compared to WT mice (114.2 µm (81.95 – 138.8) *vs.* 94 µm (72.88 – 114.20)) (p=0.172) (**Figure 4B**). In addition, with the use of MSB staining, a clear deposition of collagen was observed in the mucosa and submucosa after 3 cycles of DSS in both WT and TIMP-1 KO mice (**Supplementary figure 3C**). However, no significant difference in surface of blue staining was observed between DSS-treated WT and TIMP-1 KO mice (**Supplementary figure 3D**).

Correlation of gelatinase levels with parameters of inflammation and fibrosis.

With gelatin zymographies, we evaluated gelatinase levels in colonic samples of WT and TIMP-1 KO mice included in the acute and chronic DSS model (**Figure 5**). In the acute model, MMP-9 multimer levels were higher in DSS-treated TIMP-1 KO mice (p=0.015) compared with control mice. This was not the case in DSS-treated WT mice compared with control mice (p=0.180) (**Figure 5B**). Baseline MMP-9 multimer levels between TIMP-1 KO and WT control mice were comparable (p=0.800). Moreover, no differences were observed between DSS-treated TIMP-1 KO and WT mice (p=0.880). ProMMP-9 monomer levels were increased after DSS administration in both TIMP-1 KO (p<0.001) and WT mice (p=0.003) compared with corresponding control mice (**Figure 5C**). However, no significant difference was found between DSS-treated TIMP-1 KO and WT mice (p=1.000). ProMMP-2 levels were significantly higher in WT (p<0.001) and TIMP-1 KO (p=0.013) mice with acute colitis compared with the respective controls (**Figure 5D**). Moreover, proMMP-2 levels were significantly higher in WT mice after induction of acute colitis compared with TIMP-1 KO mice (p=0.002). The same trend was seen for activated MMP-2 levels, whereby DSS-treated WT mice had higher activated MMP-2 levels compared with TIMP-1 KO mice (p=0.040). No difference in activated MMP-2 levels was seen between control and DSS conditions in TIMP-1 KO mice (p=0.860) (**Figure 5E**). In the chronic model, MMP-9 multimer levels were significantly higher both in WT (p=0.002) and TIMP-1 KO (p<0.001) mice with DSS-induced colitis compared with control mice (**Figure 5G**). Moreover, a significant difference was seen in MMP-9 multimer levels between control WT and TIMP-1 KO mice (p=0.047). ProMMP-9 levels were significantly elevated after induction of chronic colitis in both WT (p=0.001) and TIMP-1 KO (p<0.001) mice compared with control mice (**Figure 5H**). A trend was seen for higher levels of proMMP-9 in WT mice compared with TIMP-1 KO mice after DSS administration (p=0.050). However, the variability between the samples was high. ProMMP-2 levels were only elevated in WT mice after DSS administration (p=0.006) and not in TIMP-1 KO mice (p=0.250) compared with control mice (**Figure 5I**). There was no significant difference between proMMP-2 levels from WT and TIMP-1 KO mice with chronic colitis (p=0.500). Activated MMP-2 levels were

significantly higher in DSS-treated WT (p<0.001) and TIMP-1 KO (p<0.001) mice compared with control mice (**Figure 5J**). However, no difference was found between WT and TIMP-1 KO DSS-treated mice (p=0.360). To corroborate these data at the mRNA level, the expression of all *Mmp*, *Timp* and *lipocalin-2* (*Lcn2*) genes in colonic tissue of mice included in the acute and chronic model of colitis was investigated by microarray analysis (**Supplementary figure 4**). We found that WT mice with acute DSS-induced colitis had markedly upregulated gene expression of *Mmp-3, -8, -9, -10, -13*; *Timp1* and *Lcn2* compared to TIMP-1 KO mice with acute colitis. Moreover, the gene expression of *Mmp2* was significantly higher (fold change [FC]=3.3) in WT mice after acute administration compared to TIMP-1 KO mice. No significant *Mmp*- or *Timp*-related gene expression differences were found in the chronic model. These mRNA expression data confirm the differences regarding MMP-2 found on protein level as measured with gelatin zymography.

In addition, we correlated MMP-2 and MMP-9 mRNA and protein levels with parameters of inflammation and fibrosis (**Table 1**). MMP-2 mRNA levels did not correlate with inflammation or fibrosis parameters, whereas protein levels of both activated MMP-2 and pro-MMP-2 did correlate with inflammation and fibrosis parameters. Interestingly, correlation coefficients were higher for correlations of MMP-2 (both activated and pro-MMP-2) with fibrosis parameters, compared with inflammation parameters. In case of MMP-9, mRNA levels of MMP-9 correlated with inflammation parameters only, whereas pro-MMP-9 protein levels correlated with both inflammation and fibrosis parameters. These data confirm the involvement of both MMP-2 and MMP-9 in intestinal inflammation and fibrosis.

TIMP-1 deficiency leads to differential expression of immune-related genes

Because TIMP-1 does not only inhibit MMP-9 (an inflammation-associated molecule in IBD[13,14,31]), but independently also modulates the immune system[38], it was relevant to compare the immune status at a broader molecular level. Therefore, we performed an unbiased mRNA microarray analysis. First, an unsupervised hierarchical clustering was performed of the top 50 gene probe sets with the highest

variation in expression across the 37 arrays (**Figure 6**). Two major clusters were observed. In cluster I, 2 smaller clusters could be determined wherein most of the WT (cluster Ia) and TIMP-1 KO (cluster Ib) control samples clustered together. Cluster II comprised all DSS samples. No clustering difference could be found between WT and TIMP-1 KO or between acute and chronic samples. So, after an unsupervised analysis, colonic gene expression differences were mainly found between control and DSS samples.

Next, we performed an unsupervised hierarchical clustering of the top 50 gene probe sets with the highest variation in expression after acute DSS administration (**Figure 7**). Four clusters could be discriminated: cluster I comprised of WT DSS samples, cluster II contained WT control samples, cluster III contained most of the TIMP-1 KO DSS samples and cluster IV contained TIMP-1 KO control samples. The combination of cluster I + II and cluster III + IV showed a separation of samples according to genotype. So TIMP-1 deletion in young mice resulted in significant gene expression differences in control conditions and after DSS administration compared with WT mice. We then performed an unsupervised hierarchical clustering of the top 50 gene probe sets with the highest variation in expression after chronic DSS administration (**Figure 8**). Two major clusters could be determined: cluster I contained all DSS samples and cluster II contained all control samples. Cluster II could be further subdivided into WT (cluster IIa) and TIMP-1 KO (cluster IIb) samples. This implicates that in older TIMP-1 KO mice, major gene expression differences were mainly seen in control conditions, whereas the effect of DSS on gene expression was less pronounced compared with WT mice. It is clear that by comparison of the heat maps, derived from intestinal samples of animals suffering from acute (**Figure 7**) and chronic DSS colitis (**Figure 8**), obvious differences were observed, attesting that these two models are different and result in clearly different read-outs in immune-related gene expression.

An overview of the most important gene expression comparisons between all experimental conditions is given in **Figure 9**. In WT mice, many inflammatory and MMP-related genes were differentially expressed after both acute and chronic DSS administration as described earlier[26]. In

contrast, gene expression patterns in TIMP-1 KO mice after acute DSS administration did not significantly differ from those in TIMP-1 KO control mice. Whereas after chronic DSS administration, several genes were differentially expressed in TIMP-1 KO mice compared with control mice. When gene expression profiles from WT control mice were compared with TIMP-1 KO control mice, we observed that many immune-related genes were differentially expressed in TIMP-1 KO mice (e.g. *Ido1, Saa3, Nlrc5, Cxcl9, Reg3g, Reg3b* and *Cldn8*). Older TIMP-1 KO control mice included in the chronic model did not differ from WT control mice with exception of 10 genes that were significantly upregulated (of which only 3 could be annotated to a particular gene: *Xpnpep2*, *Ces1g* and *CD177*). Comparison of gene expression levels after acute DSS administration indicated that TIMP-1 KO mice had higher levels of *Ido1*, *Gal3st3*, *Xpnpep2* and lower levels of *Mmp2*, *Mmp9* and *Cldn1* compared with WT mice. After chronic DSS administration, only 15 genes were differentially expressed in TIMP-1 KO mice compared with WT mice. Of these, only 1 could be annotated to a specific gene: *Xpnpep2*.

As a general conclusion we can state that (i) the acute and chronic DSS colitis models differ significantly in terms of immunomodulation (ii) the effects of TIMP-1 gene deletion are more pronounced in the acute than in the chronic model of DSS colitis and (iii) the gene expression signature in the chronic model is much simpler than that in the acute model, attesting a return to a compensated steady-state mode on longer term.

DISCUSSION

In this study, we aimed to investigate and to compare the effects of TIMP-1 deficiency on inflammation, remodeling and fibrosis in a murine model of acute colitis as well as in a chronic model of progressive, transmural inflammatory colitis which closely reflects the course of human CD[26]. Our initial hypothesis was that in absence of TIMP-1, one may expect more MMP activity and therefore more severe inflammation on the one hand, but more collagen degradation and less fibrosis on the other hand. The results seemed paradoxical at first sight. However, similar paradoxical effects of TIMP-1 have been described in other models of inflammation[38,39] and cancer cell invasion[40]. In support of our initial hypothesis, we found that colonic and systemic inflammation parameters were significantly higher in TIMP-1 KO mice after acute DSS administration compared with WT mice. In contrast, we observed that TIMP-1 KO mice recovered faster after acute DSS-induced colitis with lower weight loss and less disease activity compared with WT mice. The discrepancy between these observations might be due to differences in genetic background or immune response towards DSS administration (*vide supra*). In the chronic model, reduced colonic inflammation, lower tissue collagen levels and less fibrosis were observed in TIMP-1 KO mice compared with WT mice. To our knowledge, we are the first to investigate the effect of TIMP-1 deficiency in DSS-induced inflammatory colitis and fibrosis.

The importance of genetic background differences in animal models is well-known. Significant defects in regulating tissue response to environmental challenges have been described for different C57BL/6 substrains[41-46]. Therefore, we performed SNP analysis on tail DNA of TIMP-1 KO and WT mice used in our experiments. SNP analysis data indicated that TIMP-1 KO mice are on a mixed C57BL/6N and C57BL/6J background with 3 SNPs of C57BL/6N character. Intriguingly, Heiker *et al*. demonstrated that C57BL/6NTac and C57BL/6JRj substrains were significantly different in their response to high-fat diet (HFD)-induced obesity and identified four female-specific variants [rs13481014, rs13480122 (*Aplp2*), rs13478783 (*Snca*), rs4165065 (*Snap29*)] that were associated with the extent of HFD-induced weight gain and fat depot mass[41]. We found that two of these 4 SNPs

(rs13478783 (*Snca*) and rs4165065 (*Snap29*)) were also different between the TIMP-1 KO and WT mice, leading to a potential weight bias effect in TIMP-1 KO mice. Furthermore, Kern and colleagues demonstrated that standard chow fed C57BL/6NTac mice featured a significantly higher relative epigonadal fat mass compared with the C57BL/6JRj mice[42]. However, it was not clear whether the presence of 2 SNPs of C57BL/6N background in TIMP-1 KO mice would be associated with weight differences. Indeed, Lijnen *et al.* showed that on normal chow, the body weight gain and development of adipose tissue was not strikingly different for TIMP-1 KO *versus* WT mice[47]. Nevertheless, to overrule the potential intrinsic weight differences between TIMP-1 KO and WT mice, we studied the differences in organ *versus* body weight. In the acute setting, no significant differences were found in spleen/body weight or colon/body weight measurements between WT and TIMP-1 KO control mice at time of sacrifice (**Supplementary figure 5A**). However, after induction of acute colitis, TIMP-1 KO mice had significantly higher spleen/body weight and colon/body weight measurements compared to WT mice (**Supplementary figure 5A**). In contrast, spleen/body weight and colon/body weight measurements were significantly lower in TIMP-1 KO *versus* WT control mice included in the chronic model of colitis at time of sacrifice (**Supplementary figure 5B**). However, no significant differences in spleen/body weight and colon/body weight measurements were observed between WT and TIMP-1 KO mice after induction of chronic colitis (**Supplementary figure 5B**).

Previously, we studied in a longitudinal way the effects of repeated administrations of DSS and of recovery[26]. We showed a stronger induction of fibrosis with one or two additional cycles of administration of DSS each followed by a 2-week recovery period, and we further reported that only a model with repeated DSS cycles followed by a recovery period is associated with typical connective tissue changes as seen in human IBD. Moreover, with extended recovery after the last exposure, connective tissue changes prevailed in the absence of marked active inflammation, although extended recovery after 2 cycles of DSS was associated with decreased fibrosis. The current data underline the importance of inflammation as a necessary element in the development of fibrosis, although the severity of the initial acute inflammation does not correlate with the amount of

collagen deposition in the chronic setting. In acute DSS-induced colitis, the inflammation seemed to be more intense in the absence of TIMP-1, as reflected by an increased macroscopic damage score and spleen weight, although the DAI, histological inflammation score and amount of MPO positive cells tended to be lower. In chronic DSS-induced colitis, parameters of inflammation correlated with fibrosis parameters at time of sacrifice. This was apparent in DSS-treated TIMP-1 KO mice, in which lower inflammatory parameters (DAI, macroscopic damage score and histological inflammation score) were correlated with lower parameters of fibrosis (collagen content and thickness of muscularis propria). In contrast to the hydroxyprolin assay, we did not observe a significant decrease in surface of blue staining in the TIMP-1 KO mice after induction of chronic colitis. This discrepancy is probably due to sampling bias. Surface of blue staining measurements are semi-quantitative assessments in two cross-sections of the colon per mouse. However, with the hydroxyprolin assay, we measured the concentration of collagen in a piece of full bowel wall colon, including the muscular layers.

Lawrance *et al*[25] showed in a murine model of chronic inflammation that fibrosis was associated with an increase in TIMP-1 which resulted in inhibition of MMP-mediated ECM degradation. Increased TIMP-1 has also been observed in collagenous colitis again suggesting that fibrosis may be due to inhibition of ECM degradation by MMPs as well as increased ECM production per se[48]. Finally, an increased level of TIMP-1 protein has been reported in fibrotic strictures in CD[23,24]. However, one may argue that increased levels of TIMP-1 in fibrotic strictures are rather a consequence than cause, due to more MMP activity. In order to quantify gelatinase levels in our study, we performed quantitative gelatin zymography[32] and studied different forms of gelatinase A/MMP-2 and gelatinase B/MMP-9. In the acute model, higher levels of proMMP-2 and activated MMP-2 were found in WT mice compared to TIMP-1 KO mice and this was confirmed at mRNA level with microarray analysis. However, mRNA levels of TIMP-2, the major inhibitor of MMP-2, were also found to be increased (**Supplementary figure 6**). The increase in MMP-2 levels therefore seems to be balanced by increased TIMP-2 levels. After induction of chronic colitis, a trend was seen for higher proMMP-9 levels in WT

mice as compared with TIMP-1 KO mice. Lower proMMP-9 levels in TIMP-1 KO mice could be due to the fact that no TIMP-1 is present so less proMMP-9 is needed to be processed into activated MMP-9. However, no activated MMP-9 levels were detected with zymography. It needs to be mentioned that zymography is a technique that only allows to quantify levels of specific gelatinase forms, but not net gelatinolytic activities in biological samples. In order to measure activities, substrate conversion assays would be needed [32,49]. However, such tests are neither discriminative between MMP-2 and MMP-9 nor between MMP-9 monomers and trimers.

Since TIMP-1 does not only inhibit MMPs, but has an independent role in immunomodulation[38], whole genome gene expression analysis was performed to investigate the driving force behind the altered inflammatory response and attenuated development of fibrosis in TIMP-1 KO mice. Alteration of gene expression in WT mice after acute and chronic DSS administration was observed as described previously[26] with differential expression of many inflammatory and MMP-related genes. Intriguingly, no gene expression differences were found in TIMP-1 KO mice after acute DSS administration compared with control TIMP-1 KO mice. In contrast, after chronic DSS administration TIMP-1 KO mice did have altered gene expression compared with control mice. From all the collected data, we hypothesize that young TIMP-1 KO mice (included in the acute model) have a baseline inflammatory status which does not directly cause colonic inflammation, but does cause a trend for higher systemic inflammation (as measured by the spleen weight) compared with WT mice in control conditions. This results in an impaired inflammatory response after acute DSS administration, whereby no significant differences in systemic inflammation between control and DSS-induced TIMP-1 KO mice are seen, although several colonic inflammation parameters are increased. Interestingly, this effect appears to be softened as TIMP-1 KO mice become older (mice included in the chronic model).

For a long time, MMP function was thought to be limited to the breakdown of ECM components to allow tissue remodelling and growth. However, matrix degradation has biological consequences beyond the mere creation of space for cells to migrate and proliferate[12,14,38]. Unravelling the interplay between ECM deposition and chronic intestinal inflammation may booster the development of

therapies to specifically alter the fibrotic process. The net effect of TIMP deficiency, however, is not only dependent of the MMP/TIMP balance, as functional receptors that mediate downstream signaling of TIMPs[50] may provide additional keys when examining the role of MMPs and TIMPs in intestinal fibrosis. Progress in understanding fibrosis has been slow. This is largely because fibrosis is predominantly of the outer muscle layers which cannot be sampled during endoscopy. Furthermore, tissue taken from resected bowel often represents end-stage disease where early inflammatory events are no longer present[51]. Animal studies in representative models could overcome these issues. In summary, we present here for the first time the effects of TIMP-1 deficiency on inflammation and fibrosis in an acute and a chronic model of DSS colitis. Our data add to a better understanding of the biology of intestinal wound healing and fibrosis in IBD and eventually could lead to the development of more effective and more targeted therapeutic strategies for intestinal fibrosis.

FUNDING

This work was supported by a grant from the Broad Medical Research Program of the Broad Foundation (IBD-0319R). CB and MdB are supported by grants of the Agency for Innovation by Science and Technology in Flanders (IWT). GO is supported by GOA 2013/15 and GO, JC and JVA are supported by a grant from the Foundation for Scientific Research Flanders (FWO-Vlaanderen) (grant number: G077513N and G069014). IA is a postdoctoral fellow and SV, GVA and MF are Senior Clinical Investigators of FWO-Vlaanderen.

GVA reports following conflicts of interest: financial support for research from Abbvie and Ferring; lecture fee(s) from Janssen-Cilag, Merck, Abbvie and consultancy for PDL BioPharma, UCB Pharma, Sanofi-Aventis, Abbvie, Ferring, Novartis, Biogen Idec, Janssen Biologics, NovoNordisk, Zealand Pharma A/S, Millenium/Takeda, Shire, Novartis, BMS. SV reports following conflicts of interest: grant support, lecture fees and consulting fees from Abbvie, Centocor, MSD, Takeda, Pfizer, Shire, Tillotts Pharma, Hospira, Munipharma, Genentech/Roche. MF reports fees from MSD, Janssen, Abbvie,

Ferring, Chiesi, Tillotts and Zeria. GDH received consultancy fees from Genentech, Centocor and Galapagos. All other authors have no disclosures.

ACKNOWLEDGEMENTS

The authors would like to thank Greet Thijs for breeding and genotyping the mice at the animal facility of the Rega Institute for Medical Research.

All authors made substantial contributions to the submitted work. Christine Breynaert and Magali de Bruyn: conception and design of the study; acquisition, analysis and interpretation of the data; drafting the article. Ingrid Arijs: analysis and interpretation of data, drafting and critical revision of the article. Jonathan Cremer and Erik Martens: acquisition of data. Leentje Van Lommel: acquisition and analysis of data. Karel Geboes: conception of the study, acquisition of data. Gert De Hertogh: acquisition and interpretation of data. Frans Schuit, Marc Ferrante and Séverine Vermeire: critical revision of the article for important intellectual content. Jan Ceuppens, Ghislain Opdenakker and Gert Van Assche: conception and design of the study, interpretation of data, critical revision of the article for important intellectual content and final approval of the submitted version. All authors had access to the study data and approved the final manuscript. No external writing assistance was provided.

REFERENCES

1. Xavier RJ, Podolsky DK. Unravelling the pathogenesis of inflammatory bowel disease. *Nature* 2007;**448**:427-34.
2. Abraham C, Cho JH. Inflammatory bowel disease. *N Engl J Med* 2009;**361**:2066-78.
3. Van Assche G, Geboes K, Rutgeerts P. Medical therapy for Crohn's disease strictures. *Inflamm Bowel Dis* 2004;**10**:55-60.
4. Rieder F, Brenmoehl J, Leeb S, Scholmerich J, Rogler G. Wound healing and fibrosis in intestinal disease. *Gut* 2007;**56**:130-9.
5. Burke JP, Mulsow JJ, O'Keane C*, et al.* Fibrogenesis in Crohn's disease. *Am J Gastroenterol.* 2007;**102**:439-48.
6. Fiocchi C, Lund PK. Themes in fibrosis and gastrointestinal inflammation. *Am J Physiol Gastrointest Liver Physiol* 2011;**300**:G677-83.
7. Rieder F, Kessler S, Sans M, Fiocchi C. Animal models of intestinal fibrosis: New tools for the understanding of pathogenesis and therapy of human disease. *Am J Physiol Gastrointest Liver Physiol* 2012;**303**:G786-801.
8. Fichera A, Lovadina S, Rubin M*, et al.* Patterns and operative treatment of recurrent Crohn's disease: A prospective longitudinal study. *Surgery* 2006;**140**:649-54.
9. Froehlich F, Juillerat P, Felley C*, et al.* Treatment of postoperative Crohn's disease. *Digestion* 2005;**71**:49-53.
10. Penner RM, Madsen KL, Fedorak RN. Postoperative Crohn's disease. *Inflamm Bowel Dis* 2005;**11**:765-77.
11. Shelley-Fraser G, Borley NR, Warren BF, Shepherd NA. The connective tissue changes of Crohn's disease. *Histopathology* 2012;**60**:1034-44.

12. Sternlicht MD, Werb Z. How matrix metalloproteinases regulate cell behavior. *Annu Rev Cell Dev Biol* 2001;**17**:463-516.

13. Ravi A, Garg P, Sitaraman SV. Matrix metalloproteinases in inflammatory bowel disease: Boon or a bane? *Inflamm Bowel Dis* 2007;**13**:97-107.

14. Hu J, Van den Steen PE, Sang QX, Opdenakker G. Matrix metalloproteinase inhibitors as therapy for inflammatory and vascular diseases. *Nat Rev Drug Discov* 2007;**6**:480-98.

15. Gomez DE, Alonso DF, Yoshiji H, Thorgeirsson UP. Tissue inhibitors of metalloproteinases: Structure, regulation and biological functions. *Eur J Cell Biol* 1997;**74**:111-22.

16. de Bruyn M, Machiels K, Vandooren J*, et al.* Infliximab restores the dysfunctional matrix remodeling protein and growth factor gene expression in patients with inflammatory bowel disease. *Inflamm Bowel Dis* 2014;**20**:339-52.

17. Makitalo L, Kolho KL, Karikoski R, Anthoni H, Saarialho-Kere U. Expression profiles of matrix metalloproteinases and their inhibitors in colonic inflammation related to pediatric inflammatory bowel disease. *Scand J Gastroenterol* 2010;**45**:862-71.

18. Lakatos G, Hritz I, Varga MZ*, et al.* The impact of matrix metalloproteinases and their tissue inhibitors in inflammatory bowel diseases. *Dig Dis* 2012;**30**:289-95.

19. Makitalo L, Rintamaki H, Tervahartiala T, Sorsa T, Kolho KL. Serum MMPs 7-9 and their inhibitors during glucocorticoid and anti-TNF-alpha therapy in pediatric inflammatory bowel disease. *Scand J Gastroenterol* 2012;**47**:785-94.

20. Castaneda FE, Walia B, Vijay-Kumar M*, et al.* Targeted deletion of metalloproteinase 9 attenuates experimental colitis in mice: Central role of epithelial-derived MMP. *Gastroenterology* 2005;**129**:1991-2008.

21. Garg P, Vijay-Kumar M, Wang L*, et al.* Matrix metalloproteinase-9-mediated tissue injury overrides the protective effect of matrix metalloproteinase-2 during colitis. *Am J Physiol Gastrointest Liver Physiol* 2009;**296**:G175-84.

22. Sela-Passwell N, Kikkeri R, Dym O*, et al.* Antibodies targeting the catalytic zinc complex of activated matrix metalloproteinases show therapeutic potential. *Nat Med* 2012;**18**:143-7.

23. McKaig BC, McWilliams D, Watson SA, Mahida YR. Expression and regulation of tissue inhibitor of metalloproteinase-1 and matrix metalloproteinases by intestinal myofibroblasts in inflammatory bowel disease. *Am J Pathol* 2003;**162**:1355-60.

24. Graham MF, Diegelmann RF, Elson CO*, et al.* Collagen content and types in the intestinal strictures of Crohn's disease. *Gastroenterology* 1988;**94**:257-65.

25. Lawrance IC, Wu F, Leite AZ*, et al.* A murine model of chronic inflammation-induced intestinal fibrosis down-regulated by antisense NF-kappa B. *Gastroenterology* 2003;**125**:1750-61.

26. Breynaert C, Dresselaers T, Perrier C*, et al.* Unique gene expression and MR T2 relaxometry patterns define chronic murine dextran sodium sulphate colitis as a model for connective tissue changes in human Crohn's disease. *PloS one* 2013;**8**:e68876.

27. Puchtler H, Waldrop FS, Valentine LS. Polarization microscopic studies of connective tissue stained with picro-sirius red FBA. *Beitrage zur Pathologie* 1973;**150**:174-87.

28. Lendrum AC, Fraser DS, Slidders W, Henderson R. Studies on the character and staining of fibrin. *J Clin Pathol* 1962;**15**:401-13.

29. Rasband WS. Imagej. http://imagej.nih.gov/ij/, 1997-2011.

30. Woessner JF, Jr. The determination of hydroxyproline in tissue and protein samples containing small proportions of this imino acid. *Arch Biochem Biophys* 1961;**93**:440-7.

31. de Bruyn M, Arijs I, Wollants WJ*, et al.* Neutrophil gelatinase B-associated lipocalin and matrix metalloproteinase-9 complex as a surrogate serum marker of mucosal healing in ulcerative colitis. *Inflamm Bowel Dis* 2014;**20**:1198-207.

32. Vandooren J, Geurts N, Martens E, Van den Steen PE, Opdenakker G. Zymography methods for visualizing hydrolytic enzymes. *Nat Methods* 2013;**10**:211-20.

33. Descamps FJ, Martens E, Opdenakker G. Analysis of gelatinases in complex biological fluids and tissue extracts. *Lab Invest* 2002;**82**:1607-8.

34. Gentleman RC, Carey VJ, Bates DM*, et al.* Bioconductor: Open software development for computational biology and bioinformatics. *Genome Biol* 2004;**5**:R80.

35. Bengtsson H, Simpson K, Bullard J, Hansen K. Aroma.Affymetrix: A generic framework in R for analyzing small to very large affymetrix data sets in bounded memory. Feb 2008;Tech. rep. 745. Department of Statistics, University of California, Berkeley.

36. Smyth GK. Linear models and empirical bayes methods for assessing differential expression in microarray experiments. *Stat Appl Genet Mol Biol* 2004;**3**:Article3.

37. Benjamini Y, Hochberg, Y. Controlling the false discovery rate: A powerful approach to multiple testing. *J R Stat Soc* 1995:289-300.

38. Khokha R, Murthy A, Weiss A. Metalloproteinases and their natural inhibitors in inflammation and immunity. *Nat Rev Immunol* 2013;**13**:649-65.

39. Kobuch J, Cui H, Grunwald B*, et al.* TIMP-1 signaling via CD63 triggers granulopoiesis and neutrophilia in mice. *Haematologica* 2015;**100**:1005-13.

40. Chang YH, Chiu YJ, Cheng HC*, et al.* Down-regulation of TIMP-1 inhibits cell migration, invasion, and metastatic colonization in lung adenocarcinoma. *Tumour Biol* 2015;**36**:3957-67.

41. Heiker JT, Kunath A, Kosacka J*, et al.* Identification of genetic loci associated with different responses to high-fat diet-induced obesity in C57BL/6N and C57BL/6J substrains. *Physiol Genomics* 2014;**46**:377-84.

42. Kern M, Knigge A, Heiker JT*, et al.* C57BL/6JRJ mice are protected against diet induced obesity (dio). *Biochem Biophys Res Commun* 2012;**417**:717-20.

43. Rendina-Ruedy E, Hembree KD, Sasaki A*, et al.* A comparative study of the metabolic and skeletal response of C57BL/6J and C57BL/6N mice in a diet-induced model of type 2 diabetes. *J Nutr Metab* 2015;**2015**:758080.

44. Kirkpatrick SL, Bryant CD. Behavioral architecture of opioid reward and aversion in C57BL/6 substrains. *Front Behav Neurosci* 2014;**8**:450.

45. Kendall A, Schacht J. Disparities in auditory physiology and pathology between C57BL/6J and C57BL/6N substrains. *Hear Res* 2014;**318**:18-22.

46. Bryant CD. The blessings and curses of C57BL/6 substrains in mouse genetic studies. *Ann N Y Acad Sci* 2011;**1245**:31-3.

47. Lijnen HR, Demeulemeester D, Van Hoef B, Collen D, Maquoi E. Deficiency of tissue inhibitor of matrix metalloproteinase-1 (TIMP-1) impairs nutritionally induced obesity in mice. *Thromb Haemost* 2003;**89**:249-55.

48. Gunther U, Schuppan D, Bauer M*, et al.* Fibrogenesis and fibrolysis in collagenous colitis. Patterns of procollagen types I and IV, matrix-metalloproteinase-1 and -13, and TIMP-1 gene expression. *Am J Pathol* 1999;**155**:493-503.

49. Vandooren J, Geurts N, Martens E*, et al.* Gelatin degradation assay reveals MMP-9 inhibitors and function of O-glycosylated domain. *World J Biol Chem* 2011;**2**:14-24.

50. Chirco R, Liu XW, Jung KK, Kim HR. Novel functions of TIMPs in cell signaling. *Cancer Metastasis Rev* 2006;**25**:99-113.

51. Di Sabatino A, Jackson CL, Pickard KM*, et al.* Transforming growth factor beta signalling and matrix metalloproteinases in the mucosa overlying Crohn's disease strictures. *Gut* 2009;**58**:777-89.

52. Mekada K, Abe K, Murakami A, et al. Genetic differences among C57BL/6 substrains. *Exp Anim* 2009;**58**:141-9.

TABLES AND FIGURES

Table 1: Correlation of MMP-2 and MMP-9 mRNA and protein levels with parameters of inflammation and fibrosis.

	MMP-2 (mRNA)	activated MMP-2 (protein)	pro-MMP-2 (protein)	*MMP-9 (mRNA)*	pro-MMP-9 (protein)
Macroscopic damage score	ρ=0.139	ρ=0.328**	ρ=0.366***	ρ=0.459**	ρ=0.661***
Histological inflammation score	ρ=0.332	ρ=0.455***	ρ=0.495***	ρ=0.704***	ρ=0.722***
Collagen concentration (µg/2mm colon)	ρ=0.045	ρ=0.718***	ρ=0.537**	ρ=0.359	ρ=0.726***
Surface of blue staining (µm²)	ρ=0.048	ρ=0.595***	ρ=0.506***	ρ=0.287	ρ=0.543***

Non-parametric testing (Spearman's rho correlation factor [ρ]). Level of significance is indicated by *p<0.05, **p<0.01, ***p<0.001.

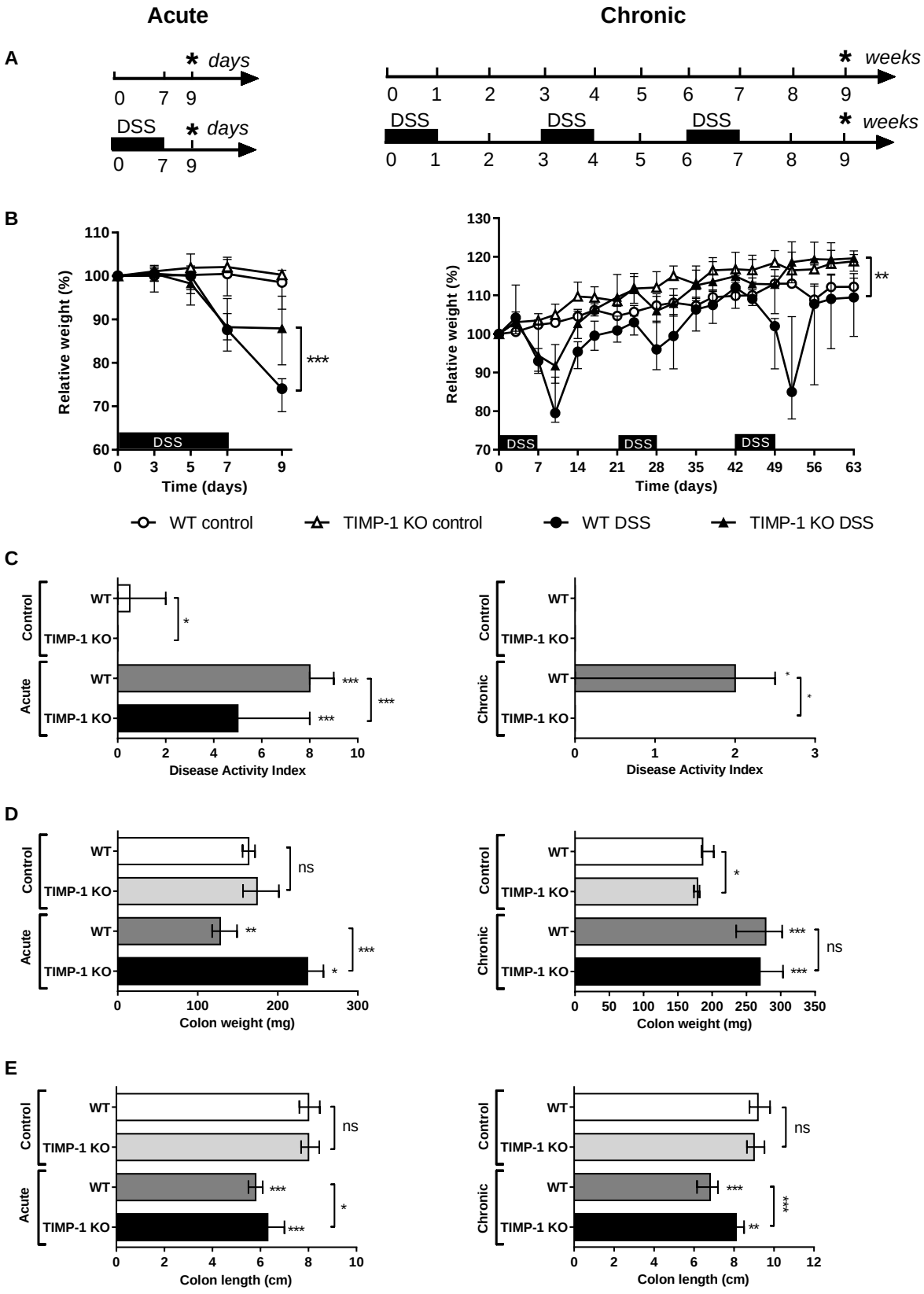

Figure 1: Experimental set-up, weight curve, disease activity index and colon read-outs.

(A) Experimental set-up. Acute colitis was induced by oral administration of DSS for 7 days in drinking water followed by 2 days of recovery before sacrifice at day 9 (*). The group of DSS exposed mice comprised WT mice (n=15) and TIMP-1 KO mice (n=15). Control mice received normal drinking water throughout (WT mice (n=12), TIMP-1 KO mice (n=13)). To induce chronic colitis, one cycle comprises 1 week of DSS followed by a recovery period of 2 weeks with normal drinking water. This was repeated three times with sacrifice at week 9 (*). The group of DSS exposed mice comprised WT mice (n=10) and TIMP-1 KO mice (n=10). Control mice received normal drinking water throughout (WT mice (n=10), TIMP-1 KO mice (n=10)). **(B)** Relative weight curve of WT and TIMP-1 KO mice in acute and chronic DSS colitis. The statistical significance between the relative weights of DSS exposed TIMP-1 KO *versus* WT mice at the end of the experiment is shown. **(C)** Disease Activity Index (DAI) of mice at the end of the experiment after acute and chronic colitis. DAI is based on three parameters: loss of weight (one point for each 5 % loss of weight), consistency of stools (normal=0, soft=2, liquid=4), and presence of gross blood in stools (0=none, 1=present). **(D)** Colon weight after removal of the faeces. **(E)** Colon length. Data are expressed as medians with IQR. Mann-Whitney *U* testing (* $p<0.05$, ** $p\leq0.01$, *** $p\leq0.001$, ns=not significant).

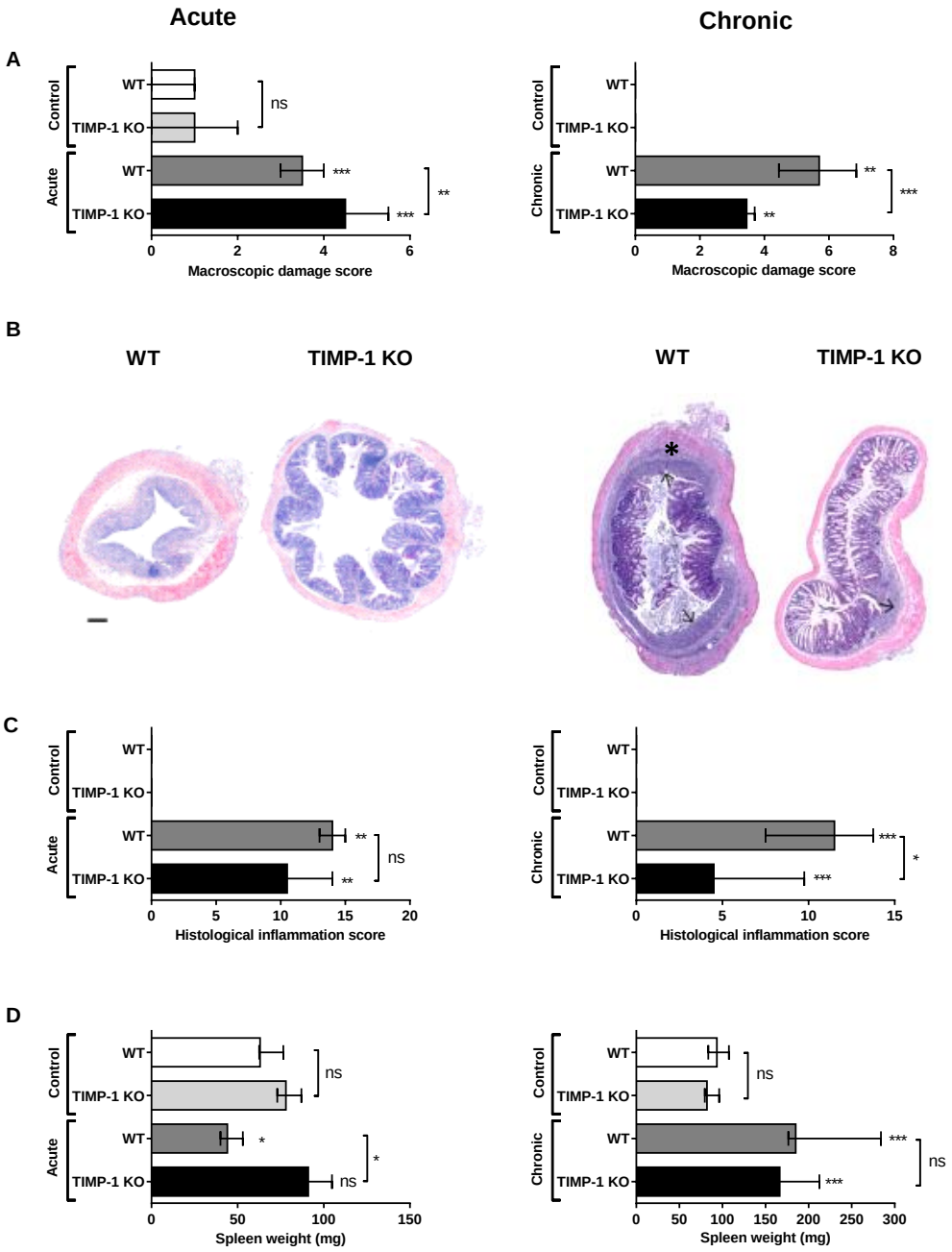

Figure 2: Macroscopic damage score and inflammation scores in acute and chronic colitis. (A) Macroscopic damage score of inflammation. **(B)** Representative H&E staining of colon sections of WT and TIMP-1 KO mice after administration of DSS (→, ulceration; *, dense mononuclear cell infiltrate in the submucosa). **(C)** Histological inflammation score. This score comprises the sum of architectural changes, neutrophil infiltration, epithelial defects, mononuclear cell infiltration and goblet cell loss. Three sections per animal were evaluated. **(D)** Spleen weight. Data are expressed as medians with IQR. Mann-Whitney *U* testing (* $p<0.05$, ** $p\leq0.01$, *** $p\leq0.001$, ns=not significant).

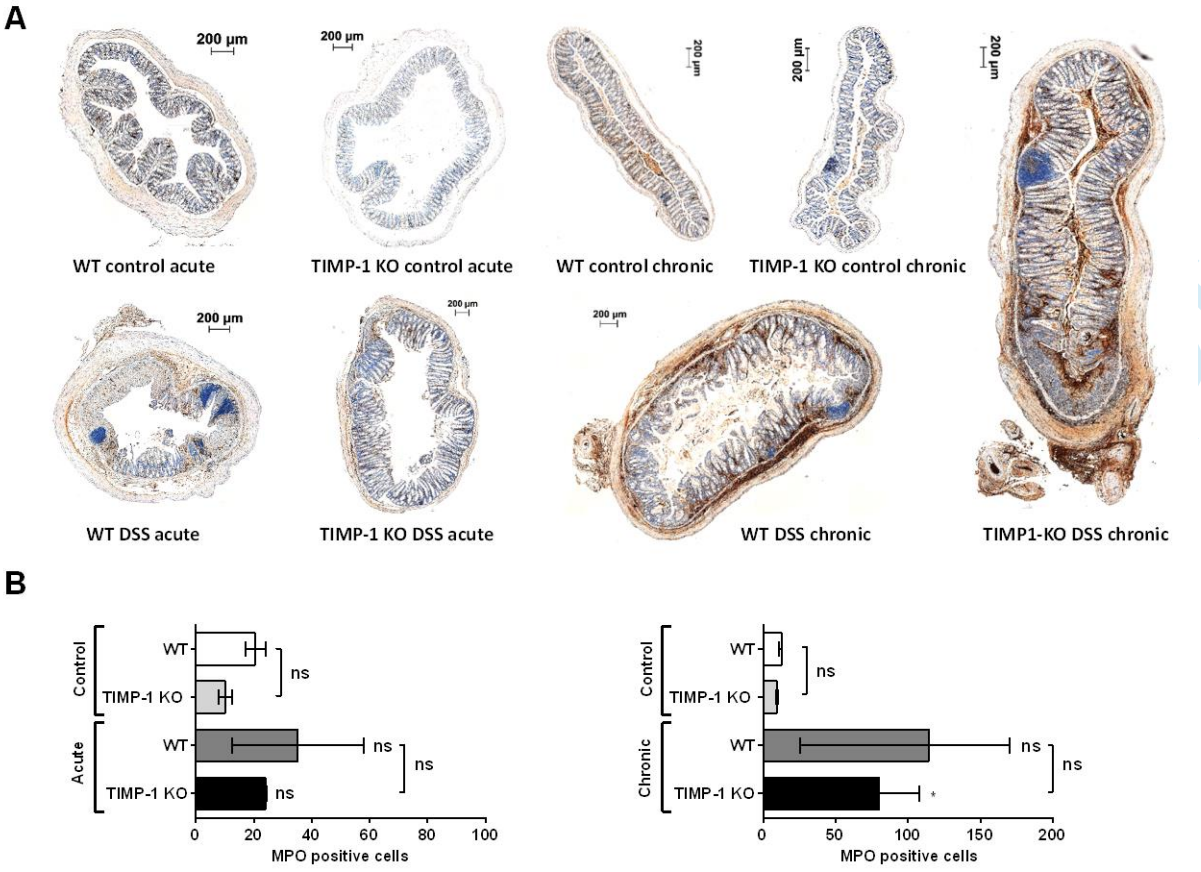

Figure 3: Myeloperoxidase (MPO) staining in acute and chronic DSS-induced colitis. (A) Representative pictures of MPO staining. **(B)** MPO positive cells were counted in 2 representative HPFs per slide (one longitudinal and one cross-section) in acute and chronic DSS colitis (acute colitis group: n=2 per group; chronic colitis group: n=3 in control condition, n=6 in DSS exposed groups). Data are expressed as medians with IQR. Mann-Whitney U testing (* $p<0.05$, ** $p\leq0.01$, *** $p\leq0.001$, ns=not significant).

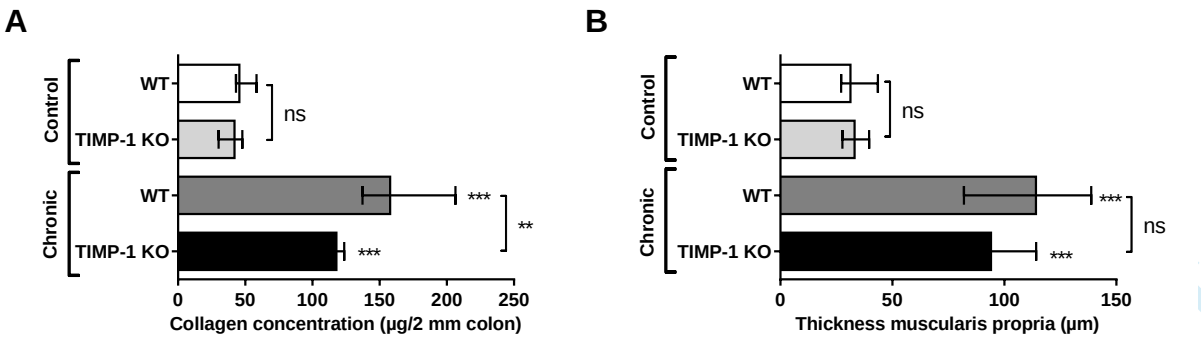

Figure 4: Fibrosis parameters in chronic DSS colitis. (A) Collagen concentration measured with a hydroxyprolin assay. Data are expressed as µg collagen per 2 mm of the most infiltrated part of the colon. **(B)** Thickness of the muscularis propria measured in µm. Data are expressed as medians with IQR. Mann-Whitney *U* testing (* $p<0.05$, ** $p\leq0.01$, *** $p\leq0.001$, ns=not significant).

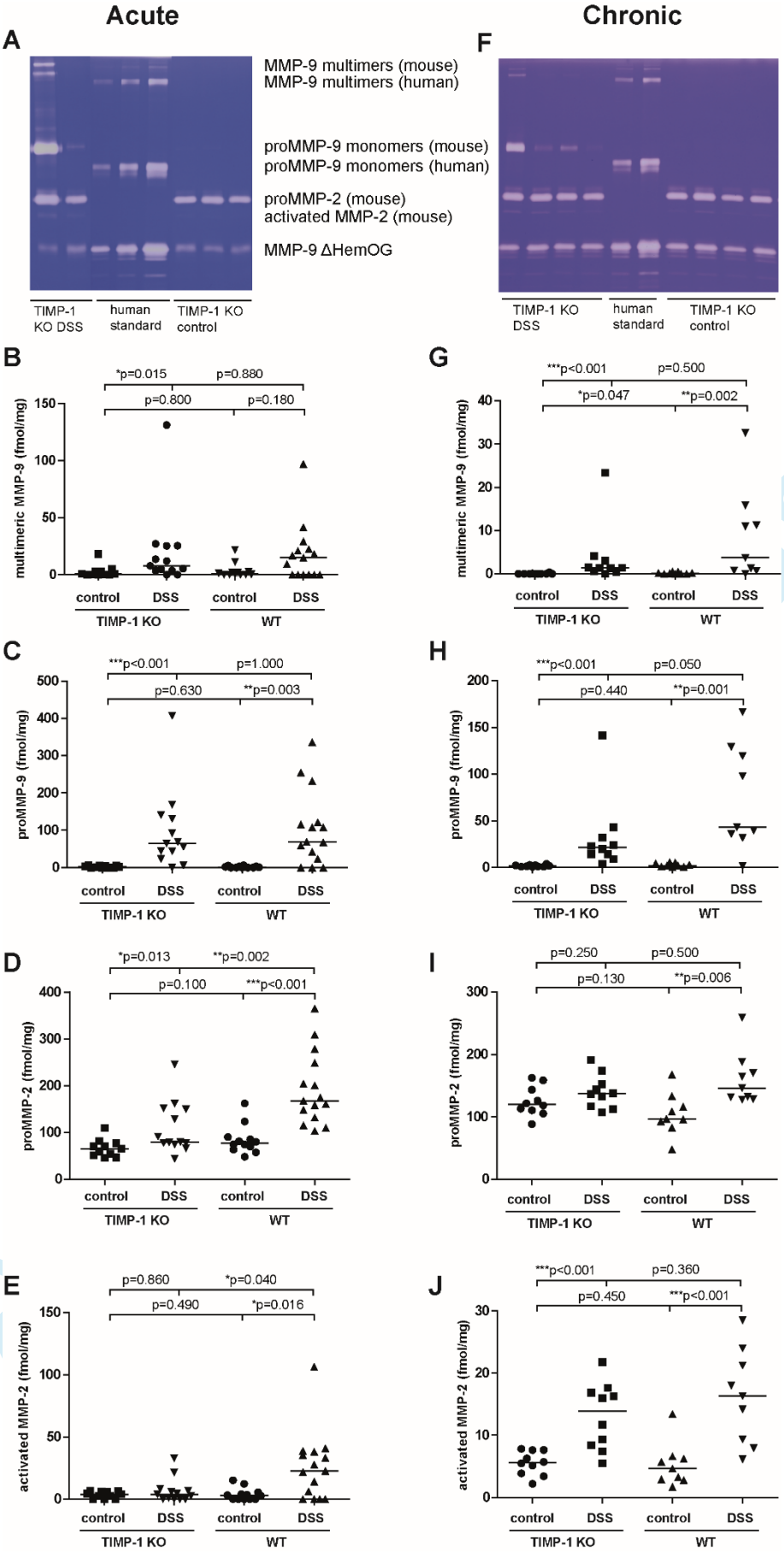

Figure 5: Gelatin zymography analysis for quantification of gelatinase A and B levels.

(A-E): Zymography analysis performed on colonic samples obtained from the acute model. (A) Key of a zymography gel with an example of 2 TIMP-1 KO DSS mouse samples, the human standard (MMP-9 multimers, proMMP-9 monomers and recombinant deletion mutant of human MMP-9 (MMP-9 ΔHemOG)) and 3 TIMP-1 KO control mouse samples. **(B-E)** Levels of MMP-9 multimers, proMMP-9, proMMP-2 and activated MMP-2 forms, respectively, in colonic tissue of TIMP-1 KO and WT mice, in control conditions and after induction of acute colitis with DSS. (**F-J): Zymography analysis performed on colonic samples obtained from the chronic model. (F)** Key of a zymography gel with an example of 4 TIMP-1 KO DSS mouse samples, the human standard (MMP-9 multimers, proMMP-9 monomers and recombinant deletion mutant of human MMP-9 (MMP-9 ΔHemOG)) and 4 TIMP-1 KO control mouse samples. **(G-J)** Levels of MMP-9 multimers, proMMP-9, proMMP-2 and activated MMP-2 forms, respectively, in colonic tissue of TIMP-1 KO and WT mice, in control conditions and after induction of chronic colitis with DSS. Mann-Whitney *U* testing (p-values are shown on the graph).

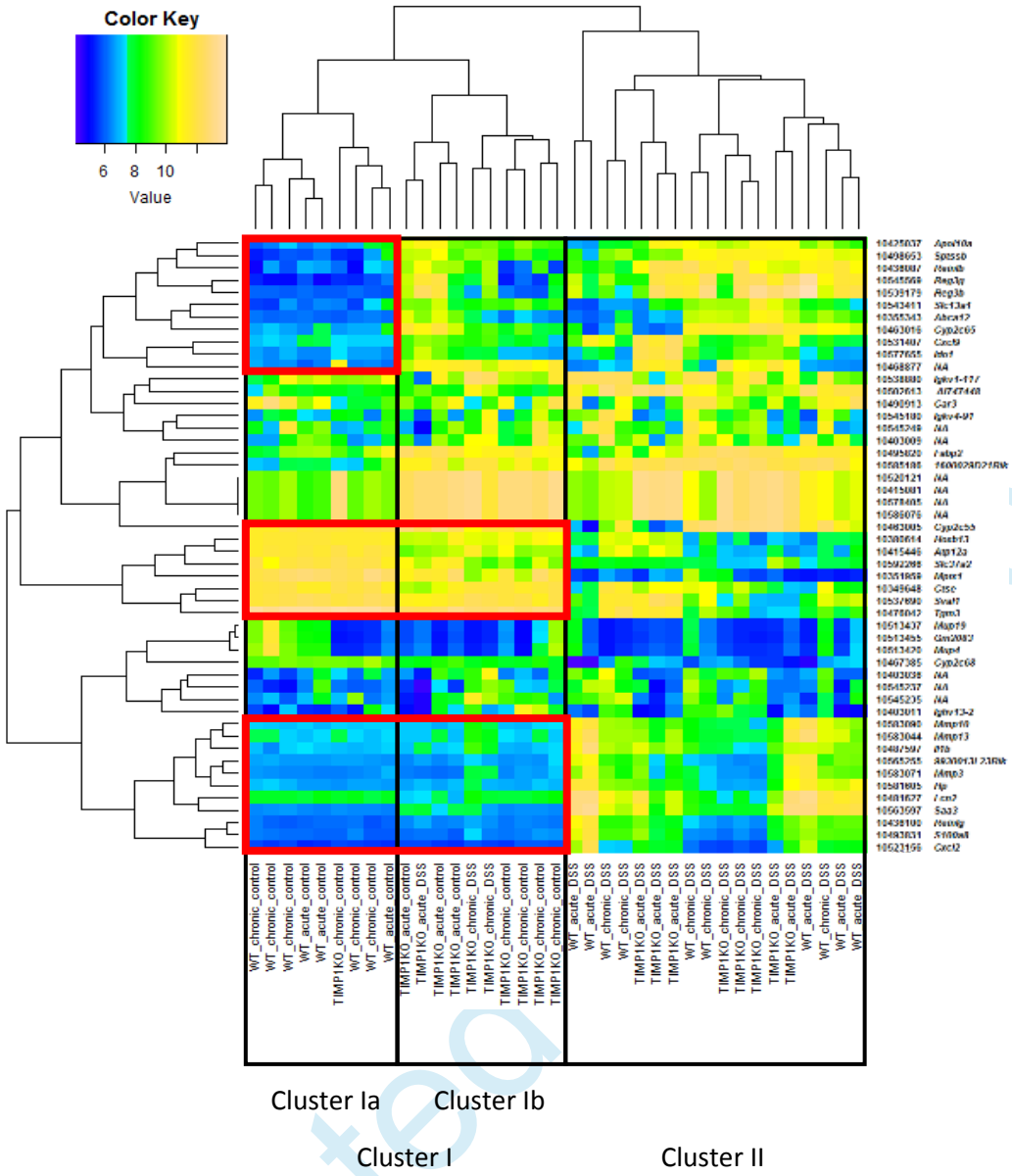

Figure 6: Microarray heatmap of the top 50 most variable genes (unsupervised complete-linkage hierarchical clustering) expressed across the 37 arrays. Two major clusters are shown. In cluster I, 2 smaller clusters were determined whereby most of the WT (cluster Ia) and TIMP-1 KO (cluster Ib) control samples clustered together with exception of 1 TIMP-1 KO chronic control sample that was misclassified into cluster Ia. Moreover, three TIMP-1 KO DSS samples were misclassified into cluster Ib. Cluster II comprised all DSS samples, although no clustering difference could be found between WT and TIMP-1 KO or acute and chronic samples. Three distinct smaller clusters of genes could be determined with major differences between WT and TIMP-1 KO control mice and control *vs* DSS mice. Gene abbreviations are explained in **Supplementary table 3**.

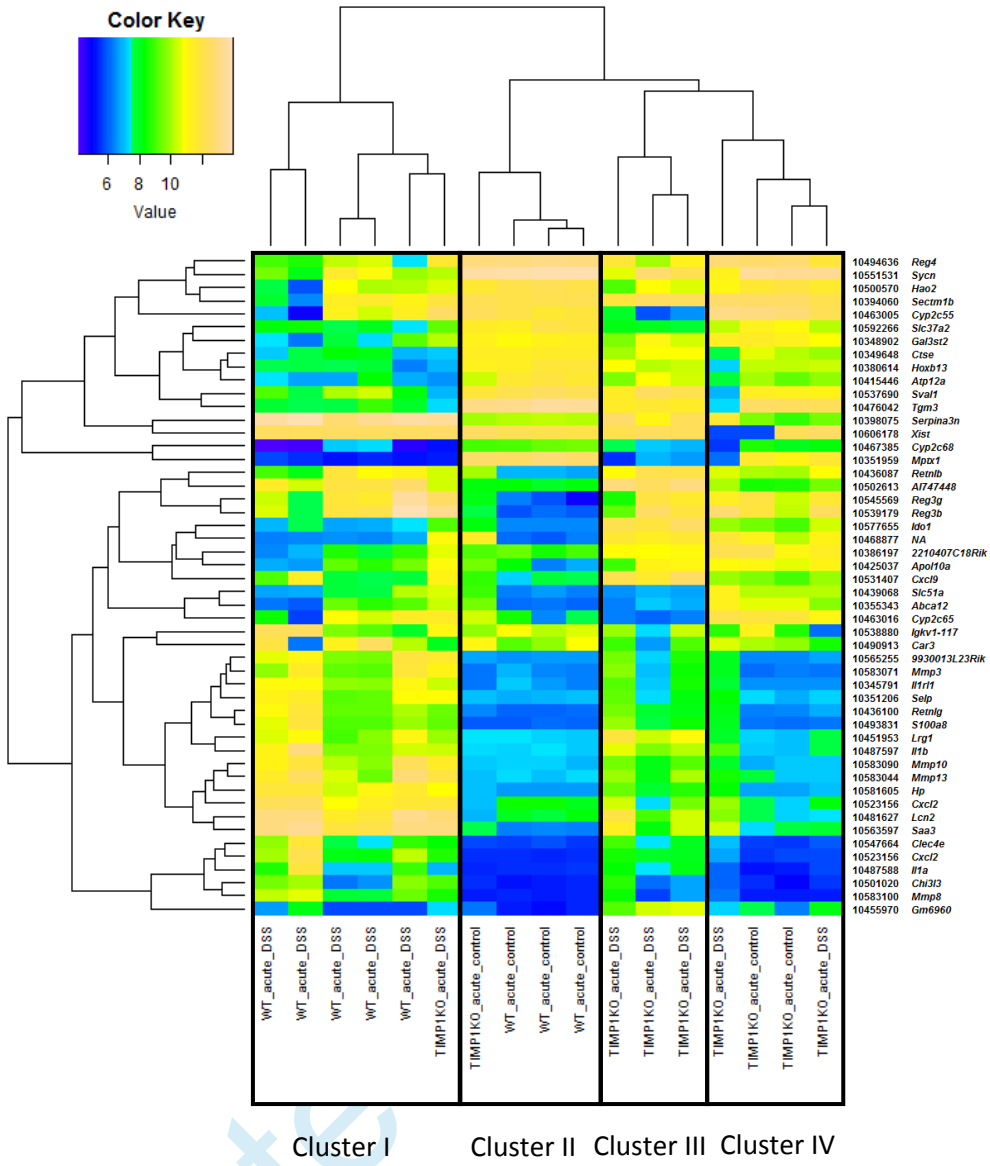

Figure 7: Microarray heatmap of the top 50 most variable genes expressed in the acute model of colitis. Four clusters were determined after unsupervised complete-linkage hierarchical clustering. Cluster I comprised of WT acute DSS samples with one misclassification of a TIMP-1 KO acute DSS sample. Cluster II contained WT acute control samples, with one TIMP-1 KO acute control sample that was misclassified. Cluster III contained most of the TIMP-1 KO acute DSS samples and cluster IV contained 2 TIMP-1 KO acute control samples and 2 TIMP-1 KO acute DSS sample. Moreover, combining cluster I + II and cluster III + IV showed a separation of samples according to genotype with the exception of 2 misclassifications of TIMP-1 KO mice in WT cluster. Gene abbreviations are explained in **Supplementary table 4**.

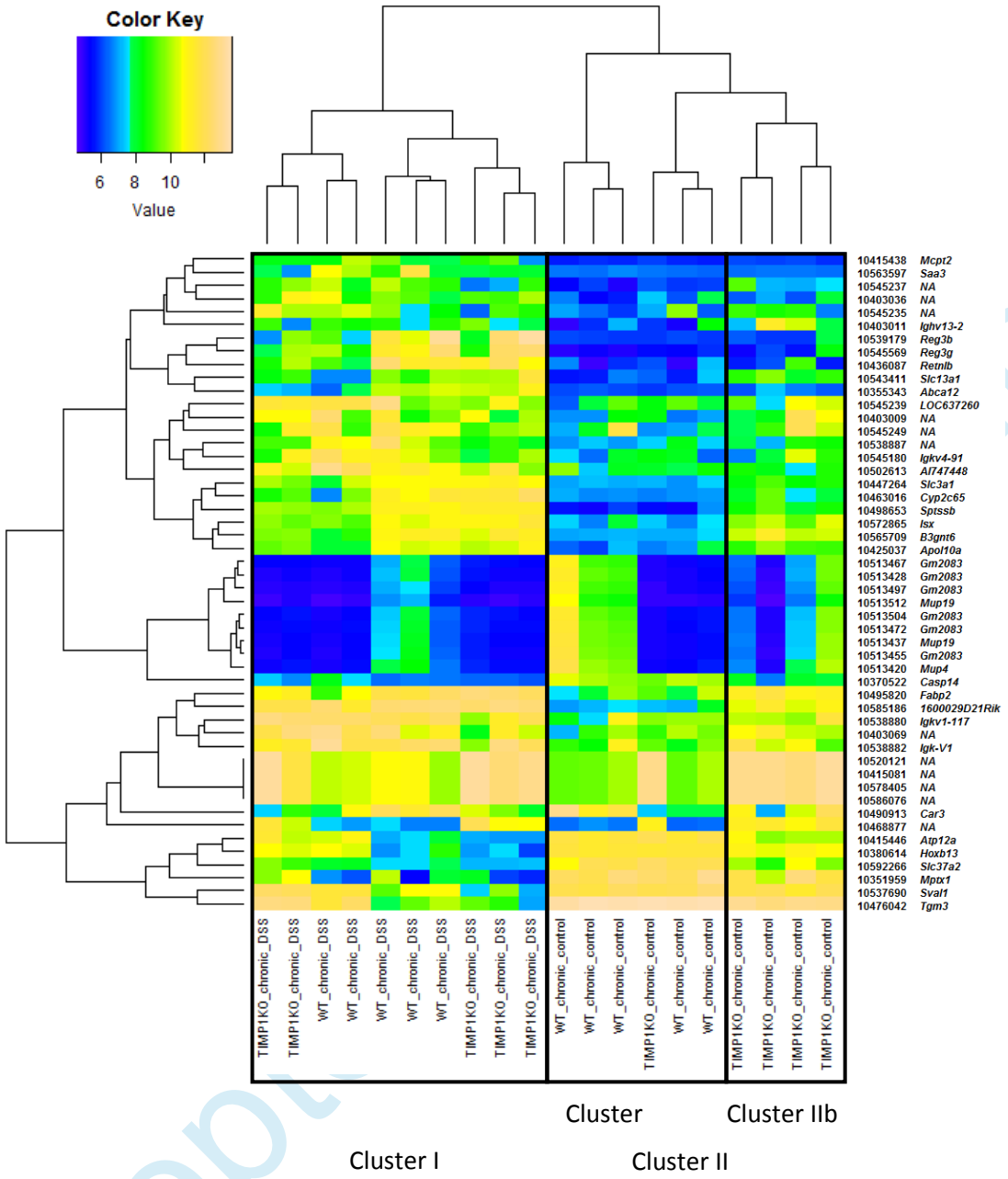

Figure 8: Microarray heatmap of the top 50 most variable genes expressed in the chronic model of colitis. After unsupervised complete-linkage hierarchical clustering of samples included in the chronic model of colitis, 2 major clusters were determined. Cluster I and cluster II were discriminated based on mice that received DSS or water, respectively. Cluster I contained samples of both WT and TIMP-1 KO mice with no clear separation of both groups. In cluster II, two subclusters could be determined. Cluster IIa contained mainly samples from WT chronic control mice, with exception of one TIMP-1 KO chronic control. Cluster IIb contained only TIMP-1 KO chronic control samples. Gene abbreviations are explained in **Supplementary table 5**.

Versus control	Significant (FDR<5%)	UP (>2 FC)	DOWN (>2 FC)
WT acute DSS	7764	594	556
WT chronic DSS	4797	301	231

Versus control	Significant (FDR<5%)	UP (>2 FC)	DOWN (>2 FC)
TIMP-1 KO acute DSS	0	0	0
TIMP-1 KO chronic DSS	2559	159	33

Versus WT control	Significant (FDR<5%)	UP (>2 FC)	DOWN (>2 FC)
TIMP-1 KO acute control	410	83	16
TIMP-1 KO chronic control	24	10	0

Versus WT DSS	Significant (FDR<5%)	UP (>2 FC)	DOWN (>2 FC)
TIMP-1 KO acute DSS	1955	251	130
TIMP-1 KO chronic DSS	32	15	0

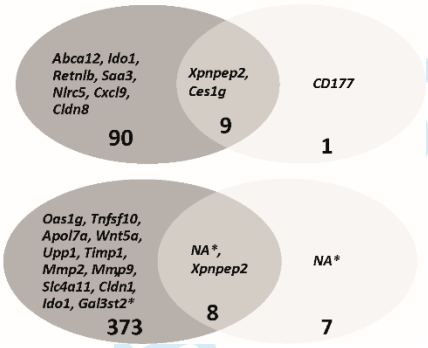

Figure 9: Comparison of gene expression profiles between WT and TIMP-1 KO mice in the acute and chronic model of colitis. First, gene expression differences after acute and chronic DSS administration compared to control conditions were investigated. Second, differences in gene expression between WT and TIMP-1 KO mice were investigated in control conditions and after DSS administration separately. Third, comparisons between WT and TIMP-1 KO mice in the acute (dark grey) and chronic (light grey) model were investigated. The overlap in genes that were differentially expressed between young and older WT and TIMP-1 KO mice is shown in the vendiagrams.

Gene abbreviations: *Abca12*, ATP-binding cassette sub-family A member 12; *Ido1*, indoleamine-pyrrole 2,3-dioxygenase; *Retnlb*, resistin like beta; *Saa3*, serum amyloid A3; *Nlrc5*, NLR family CARD domain containing 5; *Cxcl9*, chemokine (C-X-C motif) ligand 9; *Cldn8*, claudin 8; *Xpnpep2*, X-prolyl aminopeptidase (aminopeptidase P) 2, membrane-bound; *Ces1g*, carboxylesterase 1G; *CD177*, CD177 antigen; *Oas1g*, 2'-5' oligoadenylate synthetase 1G; *Tnfsf10*, tumor necrosis factor (ligand) superfamily, member 10; *Apol7a*, apolipoprotein L 7a; *Wnt5a*, wingless-type MMTV integration site family, member 5A; *Upp1*, uridine phosphorylase 1; *Timp1*, tissue inhibitor of metalloproteinase-1; *Mmp*, matrix metalloproteinase; *Slc4a11*, solute carrier family 4, sodium borate transporter, member 11; *Cldn1*, claudin 1; *Gal3st2*, galactose-3-O-sulfotransferase 2.